On the consistency in variations of the South China Sea Warm Pool as revealed by three sea surface temperature datasets

N. Li [a,b,1], S.P. Shang [a,b], S.L. Shang [a,*], C.Y. Zhang [a,b]

[a] State Key Laboratory of Marine Environmental Science, Xiamen University, Xiamen, Fujian 361005, China
[b] Department of Oceanography, College of Oceanography and Environmental Science, Xiamen University, Xiamen, Fujian 361005, China

Abstract

The areal and intensity indices of the South China Sea Warm Pool (SCSWP) derived from three datasets, the Advanced Very High Resolution Radiometer (AVHRR), Tropical Rainfall Measuring Mission's Microwave Imager (TMI) and Optimum Interpolation Version 2 (OI.v2) sea surface temperature (SST), are generally consistent with each other at monthly, seasonal and interannual scales. However, the three records are different in some cases. First, minor differences among the monthly records of intensity index are observed in the period July to September. Secondly, the interannual records of SCSWP intensity derived from AVHRR and OI.v2 are different in autumn during the period 1990–1996. The reason is not yet clear and nor is it clear which record best represents fluctuations in SCSWP intensity. These suggest that various drawbacks of the three datasets, such as low resolution of OI.v2, and cloud and rain contamination on AVHRR and TMI data, would be serious enough to allow deviation from each other to appear. Merging AVHRR and TMI SST data might be the way leading to a more convincing time series of SCSWP. In addition, changes of areal and intensity indices are not always consistent with each other, for example, they have different monthly patterns. Although the three interannual records of intensity index in three seasons all capture the main Multivariate ENSO Index (MEI) signals at a half-year lag, only those which are in the summer significantly correlated with MEI.
© 2007 Elsevier Inc. All rights reserved.

Keywords: AVHRR; TMI; OI.v2; Remote sensing; Sea surface temperature; Index; Variation; South China Sea Warm Pool; ENSO

1. Introduction

The surface water from the tropical eastern Indian Ocean to the tropical western Pacific Ocean, the warmest (approximately 28 °C) on the Earth, is frequently referred to as the Indo-Pacific Warm Pool (Huang & Mehta, 2004; Mehta & Fayos, 2004; Weier, 2001). Numerous studies have indicated that the warm pool may have a strong impact on the climate of surrounding lands (e.g., Barlow et al., 2002; Chen & Qian, 2005; Hoerling & Kumar, 2003; McGregor & Gagan, 1999; Weier, 2001). Its fluctuations in size and intensity may be linked with the intensity of El Niño (Mehta & Mehta, 2004; Sun, 2003; Weier, 2001; Yu et al., 2002), and it may further influence the

ecosystem in terms of movement of tuna fishing grounds (Lehodey et al., 1997, 2003).

In the middle of the Indo-Pacific Warm Pool there is the South China Sea. During most of the year, warm water with SST ≥ 28 °C occupies the SCS, forming the South China Sea Warm Pool (SCSWP) (He & Guan, 1999; Jia et al., 2000; Liu et al., 2002; Wang, 2003). It has been suggested that the SCSWP affects the outburst of the summer monsoon in the SCS and thus influences the climate of China, and even the entire East Asia to a great extent (Zhao & Chen, 2001). Thus, the temporal pattern in the size and intensity of the SCSWP may be an important index representing local climate–ocean fluctuations in the SCS. To know the pattern of such an index will help to interpret ecosystem fluctuations in response to local and remote forcing on a long-term scale in the SCS and its adjacent seas. The South China Sea (SCS) is one of Earth's major marginal seas: its basin, an area of 3.7 million km^2, is as deep as 5000 m and is bordered by broad shallow shelves (Fig. 1). In the
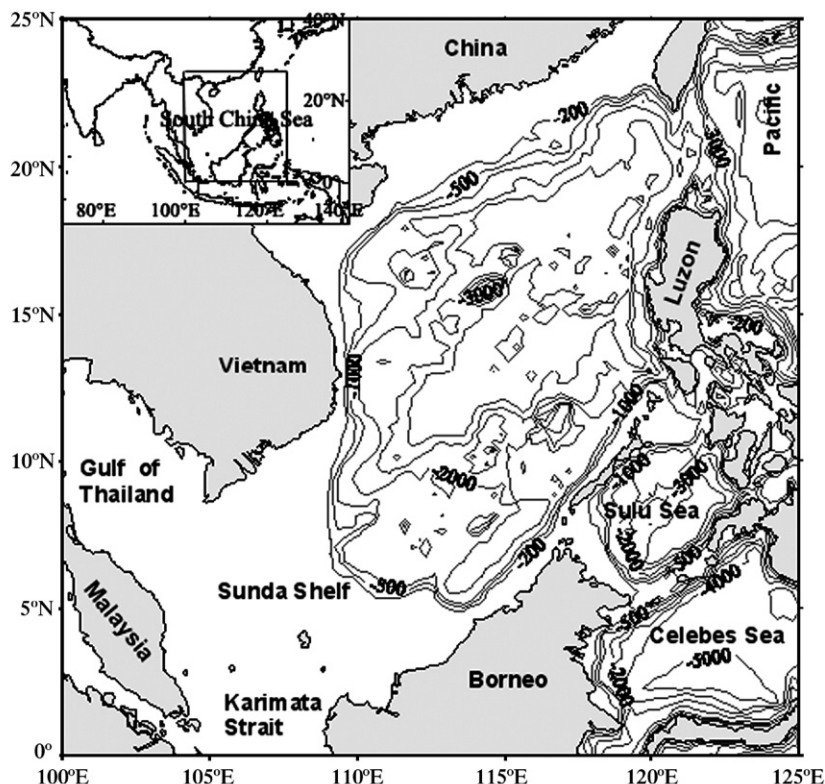
Fig. 1. Bathymetry of the South China Sea.

SCS, the northeast monsoon prevails in winter while the southwest monsoon prevails in summer. In the transitional seasons, spring and autumn, wind direction is more variable (Wyrtki, 1961). In response to the alternating prevalent monsoons, the surface circulation changes with the season. A cyclonic gyre forms in winter, while during the summer there are a cyclonic gyre north of about 12°N and an anticyclonic gyre south of it (Qu, 2000; Shaw & Chao, 1994; Wyrtki, 1961). Localized upwelling is driven by the circulation gyres off Vietnam during the summer monsoon and off the Sunda Shelf and western Luzon during the winter monsoon (Chao et al., 1996; Shaw et al., 1996; Udarbe-Walker & Villanoy, 2001). A strong northeastward current advects the cold upwelling water off Vietnam into the open SCS, inducing a basin-wide mid-summer cooling (Xie et al., 2003).

Several reports concerning the seasonal and interannual variability of the SCSWP were on the basis of optimum interpolation sea surface temperature (OISST) and National Oceanographic Data Center (NODC) LEVITUS World Ocean Atlas temperature data. He and Guan (1999) pointed out that the SCSWP was strong in summer but weak in winter by analyzing the temperature distribution in the SCS basin at 20-m depth. Using OISST (1982–1997) and LEVITUS (1994) data, Zhao and Chen (2001) reported that the area and intensity of the SCSWP showed a different seasonal pattern from those of the Indian Ocean Warm Pool (IOWP) and the Western Pacific Warm Pool (WPWP); at an interannual scale, the SCSWP co-oscillated with the IOWP and WPWP with a half-year time lag. Based on LEVITUS (1982) data, Jia et al. (2000) concluded that

the annual cycle of the SCSWP included four stages and analyzed the mechanism driving such a cycle by developing a model. The volume of the SCSWP was reported to peak in July according to the LEVITUS (1994) data (Zhang et al., 2001). As the SCSWP mostly retreats from the SCS in winter (SST is below 28 °C over most of the SCS in winter), the SCS has been viewed as a gap in the Indo-Pacific Warm Pool (Liu et al., 2004). Such a gap was suggested to be created by a cold tongue resulting from the cold advection of the southward western boundary current along the continental slope between the Sunda Shelf and the deep SCS to the east. The cold tongue was found to display large interannual variability in association with ENSO by defining and calculating a South China Sea cold tongue index based on the National Oceanic and Atmospheric Administration (NOAA) OI.v2 SST data (Liu et al., 2004).

All of these studies used reanalyzed data to derive a time series of either temperature or warm pool/cold tongue index. The reanalyzed data were produced by synthesizing remote sensing and mooring data with models, which are coarse in resolution and whose monthly root–mean–square (RMS) differences are very high in regions with sparse data and high gradient (Reynolds et al., 2002). One of the reanalyzed datasets, OI.v2 SST, which is an update of OISST, has a relatively small global residual bias of roughly −0.03 °C (Reynolds et al., 2002). AVHRR and TMI are two satellite sensors measuring SST. AVHRR SST data have accumulated for nearly 20 years, with its high resolution being one advantage when applied to research in marginal seas such as the SCS (Kilpatrick et al., 2001). The disadvantage of AVHRR is its contamination by

cloud cover. The TMI is a new sensor which can measure SST through clouds. Thus, it has the distinct advantage of substantially improving the measurement of SST over cloudy regions like the SCS (Wentz et al., 2000; Xie et al., 2003). Nevertheless, it is subject to microwave contamination from the land while approaching the coast, and no data are available under rainy conditions. It is not yet clear, due to various drawbacks, whether the reanalyzed and remote sensing data, when they are applied to study the temporal variability of the SCSWP, will be consistent with each other and which will be the most convincing. We believe that it is worthwhile to examine if there is any difference in the pattern of SCSWP variability produced using reanalyzed data or solely using a remote sensing dataset. A detailed comparison is necessary also between the changes of size and intensity of the SCSWP on different time scales in order to derive a representative time series for the SCSWP index. Thus, in this paper, we will compare the monthly, seasonal and interannual variability in the areal and intensity indices of the SCSWP based on three datasets: the AVHRR SST, TMI SST and OI.v2 SST. Our target is to see if any differences arise by using different datasets and if there are any differences in size and intensity variability. Suggestions will be given regarding one representative time series for the SCSWP index. Results presented in this paper are expected to help characterize local scale climate–ocean interactions for subsequent research on ecosystem responses to climate–ocean fluctuations.

2. Data and methods

We use a monthly SST product of AVHRR for the period January 1985 to May 2003 at resolutions of 9 km, of TMI available for the period December 1997 to April 2005 on a 0.25° grid, and of OI.v2 from December 1981 to June 2005 on a 1° grid. The best SST product of AVHRR during nighttime was chosen in order to avoid the short-period SST variations resulting from the heating of thin surface layers (Nezlin & McWilliams, 2003). A monthly climatology of SST and a seasonal mean SST in each year are further constructed for these three datasets, respectively, and are used for the following calculation of SCSWP areal and intensity indices.

Following Zhao and Chen (2001), an areal index (ArI) and an intensity index (InI) for the SCSWP are defined. Pixels with SST ≥ 28 °C are considered as warm pool pixels according to convention. The area (A) and intensity (I) of the warm pool are defined as

$$A = N \tag{1}$$

$$I = \sum M_i Q_i (i = 1 \sim 3) \tag{2}$$

where N refers to the total number of warm pool pixels within the SCS (100°–122°E, 0°~25°N); M refers to the number of warm pool pixels of specific SST range (i) and Q is a weighted factor; when 28 °C $\leq$ SST$<$29 °C, $i=1$, $Q=1$; when 29 °C $\leq$ SST$<$30 °C, $i=2$, $Q=2$; when SST$\geq$30 °C, $i=3$, $Q=3$. A monthly climatology of ArI and InI and a seasonal mean ArI

and InI in each year are thus obtained by calculating the A and I anomaly and normalizing by their RMS variance as below:

$$\text{ArI}_j = \left(A_j - \frac{1}{n} \sum_{j=1}^{n} A_j \right) \Bigg/ \sqrt{\frac{1}{n} \sum_{j=1}^{n} \left(A_j - \frac{1}{n} \sum_{j=1}^{n} A_j \right)^2} \tag{3}$$

$$\text{InI}_j = \left(I_j - \frac{1}{n} \sum_{j=1}^{n} I_j \right) \Bigg/ \sqrt{\frac{1}{n} \sum_{j=1}^{n} \left(I_j - \frac{1}{n} \sum_{j=1}^{n} I_j \right)^2} \tag{4}$$

where j is a specific month or year and n refers to the number of months or years each A and I dataset covers. It should be noted that we only calculate indices for spring–autumn (March–November), since warm water (SST ≥ 28 °C) is rarely found in the SCS in winter (Fig. 2), leading to formation of a gap in the Indo-Pacific Warm Pool (Liu et al., 2004). For simplification, ArI values derived from AVHRR, TMI and OI.v2 are annotated as A-ArI, T-ArI and O-ArI, respectively. The same applies to InI values.

In addition, a monthly climatology of total cloud amount on a 2.5° grid from the International Satellite Cloud Climatology Project (ISCCP) and a monthly climatology of northeast component of wind stress derived from QuikSCAT observed wind data are also used. The record of the occurrence of El Niño events is inferred from the overlapping bimonthly mean Multivariate ENSO Index (MEI) promulgated by the Climate Diagnostic Center of NOAA (http://www.cdc.noaa.gov/people/klaus.wolter/MEI/table.html). Surface heat fluxes, including shortwave radiation flux (Q_{short}), longwave radiation flux (Q_{long}), latent heat flux (Q_{lat}) and sensible heat flux (Q_{sen}), originated from the Japanese Ocean Flux datasets with Use of Remote sensing Observations (J-OFURO) for the period January 1992 to November 1995 (Kubota et al., 2002), are used to calculate the net surface heat flux (Q_{net}) on a 1° grid as below (Hayes et al., 1991),

$$Q_{\text{net}} = Q_{\text{short}} - Q_{\text{long}} - Q_{\text{lat}} - Q_{\text{sen}} \tag{5}$$

3. Results and discussion

Results of SCSWP temporal pattern are thus obtained, which include monthly climatologies of ArI and InI derived from three SST datasets, and seasonal mean ArI and InI in each year for the period 1982–2004 derived from OI.v2 SST, for 1985–2002 from AVHRR SST and for 1998–2004 from TMI SST. These patterns appear stochastic as demonstrated by auto-correlation values (results not shown).

3.1. Monthly and seasonal variability

3.1.1. Comparison of ArI among different datasets
Fig. 3a shows the seasonal and monthly pattern of ArI using AVHRR, TMI and OI.v2 data. They appear highly consistent with each other as demonstrated by the cross correlation coefficients of >0.98 (Table 1). ArI peaks in summer, while it is lower in spring than in autumn. The minimum ArI appears in
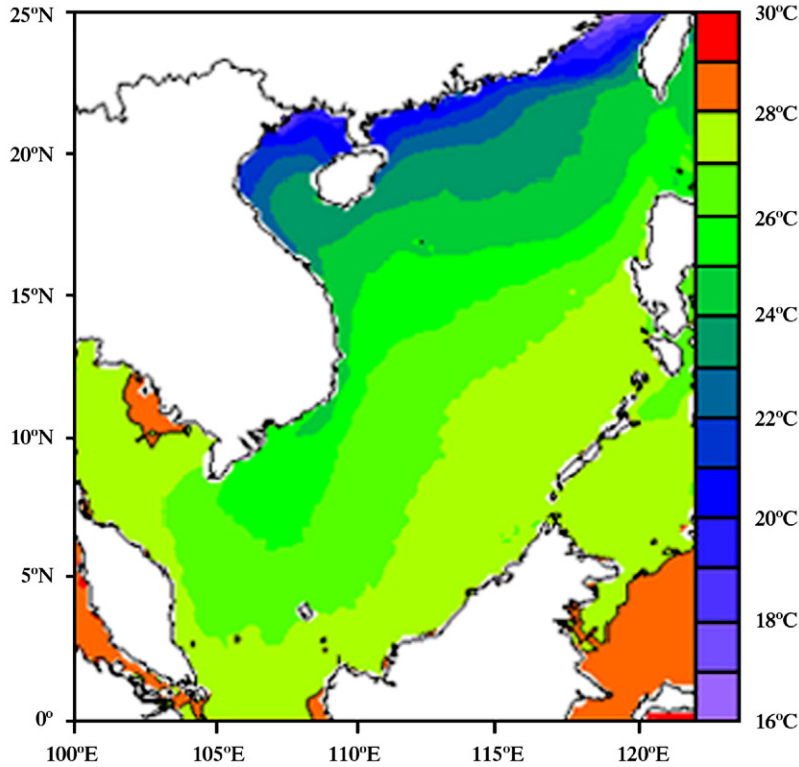
Fig. 2. Distribution of AVHRR SST in winter for the period 1985–2002, where the orange region refers to the warm water with SST ≥ 28 °C.

March. A rapid increase of ArI occurs in April and May, corresponding to a jump of the SCSWP to the northern portion of the SCS basin in April (Zhang et al., 2001). Little change occurs from June to September, while a tiny peak can be observed in July and August. Although the coastal upwelling off south Vietnam and the subsequent open-ocean cooling are prominent in July and August (Xie et al., 2003), their SSTs are generally equal to or higher than 28 °C so that the ArI is not reduced compared to June. This pattern is similar to observa-tions made on the basis of OISST and LEVITUS datasets (Zhao & Chen, 2001).

The number of cloudy pixels is >75% of the whole pixels over the SCS in July and even higher in August (Fig. 4a). However, this seems not to affect the monthly and seasonal patterns of A-ArI. It suggests that the effect of cloud cover on AVHRR may be overcome by using multiyear monthly mean SST when accounting for the areal change of the SCSWP. It also looks like that coast and rainy pixels missing from the TMI
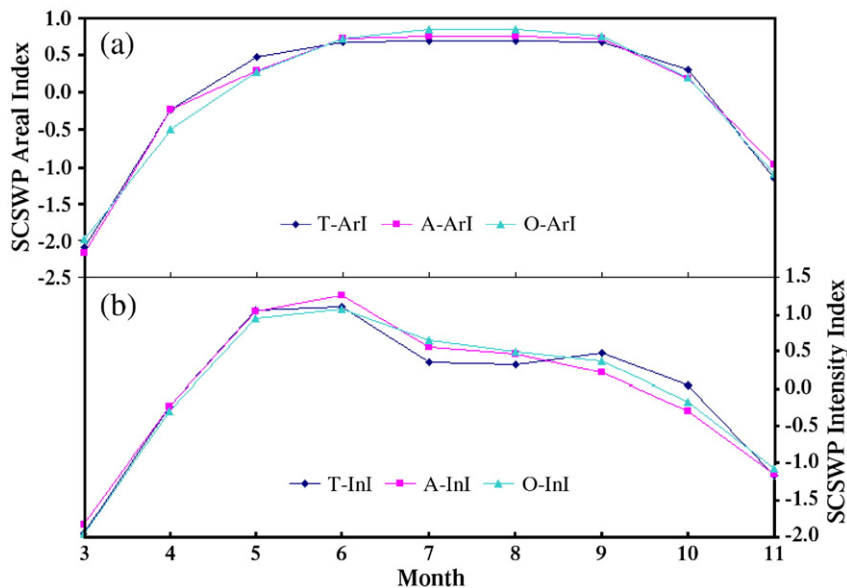

Fig. 3. Monthly SCSWP areal index (a) and intensity index (b) derived from AVHRR, OI.v2 and TMI from March to November.

Table 1
Cross correlation coefficients of monthly SCSWP indices among TMI, AVHRR and OI.v2 (0.632 is 95% significant for 8 degrees of freedom)

	T-ArI	A-ArI	O-ArI		T-InI	A-InI	O-InI
T-ArI	1	0.994	0.988	T-InI	1	0.981	0.987
A-ArI	0.994	1	0.992	A-InI	0.981	1	0.992
O-ArI	0.988	0.992	1	O-InI	0.987	0.992	1

dataset do not produce significant difference between the monthly pattern of T-ArI and those of the other two ArIs.

3.1.2. Comparison of InI among different datasets

Similar to ArI, seasonal and monthly patterns of InI derived from the three datasets are nearly identical, having cross correlation coefficients which are significant at the 95% level based on a *t*-test (Fig. 3b and Table 1). They all peak in May to June and have a sharp drop in July. Minor difference among them occurs in the period July to September, when a slightly increasing trend in T-InI contrasts to a gradual decreasing trend in A-InI and O-InI. The patterns of A-InI and O-InI are relatively close to that derived from LEVITUS dataset (Zhao & Chen, 2001).

Fig. 4b shows the J-OFURO net air–sea heat flux (Q_{net}) over the SCS basin during the period from March to November. Q_{net} peaks in May and is slightly lower in July than in August, probably associated with the peak of solar radiation in April and July over the SCS. Three InIs seem not significantly correlated with the heat flux except A-InI at zero time lag (Table 2).

Table 2
Lag correlation coefficients between Q_{net} and InIs at monthly scale (0.632 is 95% significant for 8 degrees of freedom; values greater than 0.632 is boldfaced to emphasize statistical significance)

Lag (month)	T-InI	A-InI	O-InI
−5	−0.029	−0.113	−0.074
−4	0.068	0.014	0.047
−3	0.030	0.044	0.079
−2	0.124	0.160	0.173
−1	0.457	0.471	0.446
0	0.617	**0.652**	0.603

Change of seasonal circulation in response to monsoonal forcing may be important in mediating the pattern of the SCSWP intensities in addition to the change of heat flux. It is thus not easy to judge what induces the minor deviation of T-InI monthly record from A-InI and O-InI.

3.1.3. Comparison between ArI and InI

Fig. 3 obviously shows that the ArI has a different pattern from the InI. Although both show an abrupt increase in April and both decline in October, their changes differ from each other during the period May to August. Taking AVHRR data as an example, the peak time of InI is in May to June while that of ArI is from June to September. This means that in June when the SCSWP has reached its maximum intensity, it has almost enlarged to its maximum size. However, in the period July to September, when its intensity has declined, its size stays large
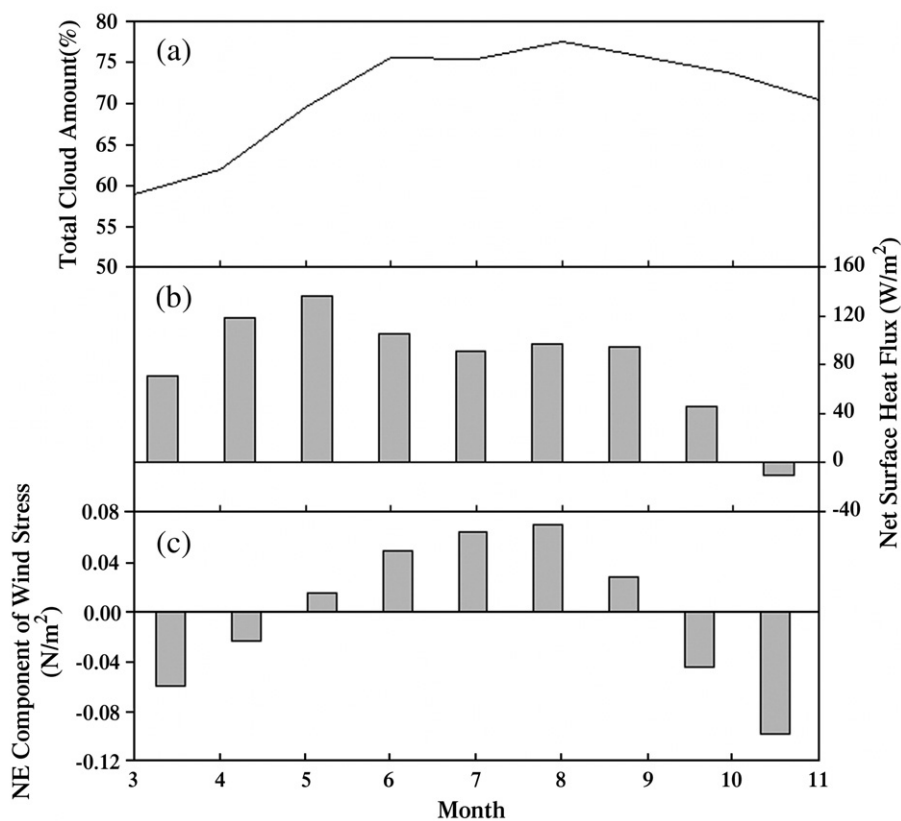

Fig. 4. Monthly variation of total cloud amount (a), net surface heat flux (b) and wind stress (c) over the SCS; positive values of the NE component of wind stress represent southwest monsoon according to convention.

Table 3
Cross correlation coefficients between ArIs and InIs at interannual scale (0.707, 0.456 and 0.404 are 95% significant for 6 (TMI: 1998–2004), 17 (AVHRR: 1985–2002) and 22 (OI.v2: 1982–2004) degrees of freedom, respectively)

	TMI	AVHRR	OI.v2
Spring	0.802	0.936	0.939
Summer	0.351	0.709	0.599
Autumn	0.905	0.939	0.917

Table 4
Cross correlation coefficients between O-InI and T-InI for the period 1998–2004 and between O-InI and A-InI for the period 1985–2002 at interannual scale (0.707, 0.456 are 95% significant for 6 (1998–2004), 17 (1985–2002) degrees of freedom, respectively)

	Spring	Summer	Autumn
O-InI ~ A-InI	0.938	0.926	0.860
O-InI ~ T-InI	0.855	0.986	0.944

and becomes even larger in July and August. Such a difference is probably associated with the difference in the phase of solar radiation and the monsoon, and the basin-wide cooling associated with the upwelling off Vietnam during summer (Xie et al., 2003). The decreasing of solar radiation in July to August plus the upwelling cooling will disrupt the warming of the SCS and thus the decrease in the intensity of the SCSWP. However, during this period the southwest monsoon is at its strongest in the year (Fig. 4c) and thus the SCSWP may have been pushed further to the north.

3.2. Interannual variability

3.2.1. Comparison between ArI and InI

For all three datasets, ArI fluctuates from year to year in spring and autumn quite in accordance with InI, both in trend and magnitude (Table 3, figures not shown). The case of summer appears a little bit different (Table 3 and Fig. 5). For example, the magnitude of change is bigger for O-InI than for O-ArI and it seems that they do not vary in step with each other (Fig. 5c). This is thought to be mainly induced by the effect of coarse resolution of OI.v2 data on the index computation. Coarse resolution may result in missing of pixels of SST $\geq 28\,°C$, leading to more serious underestimation of InI than ArI due to the weighting factor applied to InI computation. This impact exists in each season but may be the strongest in summer when SST is the highest (SCS spatial mean SST is 29.14 °C in summer, and is 28.04 °C and 28.28 °C in spring and autumn, respectively).

3.2.2. Comparison of InI in each season among different datasets

Next we compare the interannual pattern of InI in the SCSWP in each season derived from the three datasets. Com-
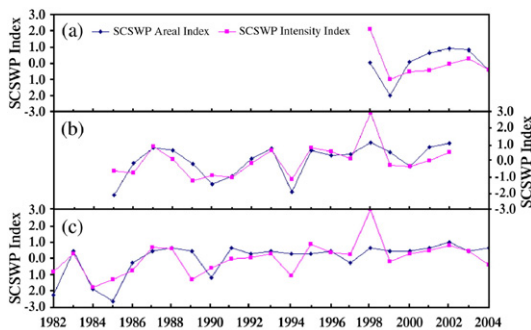
parison will be based on the overlap years which are available. In detail, comparison between AVHRR and OI.v2 is for the period 1985 to 2002/2003, and that between TMI and OI.v2 is for the years 1998 to 2004.

The correlation coefficients between O-InI and A-InI and between O-InI and T-InI in each season are all greater than the values which are 95% significant based on a *t*-test (Table 4). That is to say, the three InIs highly correlate with each other at interannual scale, demonstrating that the three InIs generally show identical patterns of interannual variation.

Detailed comparison of the patterns shows pieces of evidence supporting the statistical results, but also reveals some disagreement among the indices. In spring (Fig. 6a), three InIs altogether peak in 1998 and 2001; one more peak of A-InI and O-InI occurs in 1988. In summer (Fig. 6b), all the three InIs show a unique crest in 1998. In autumn (Fig. 6c), a common peak in 1998 for three InIs appears; A-InI and O-InI have a strong peak in 1987. It is noted that T-InI and O-InI show one more peak in 2001 while A-InI does not; in particular, in the period 1990–1996, the patterns of A-InI and O-InI are different, and fluctuation of O-InI is greater than A-InI. These differences seem unlikely to have arisen from the cloud cover artifact of AVHRR because cloudy pixels of AVHRR in 1990–1996 and 2001 are not more than that in other years (data not shown). On the other hand, coarse resolution of OI.v2 in biasing the index values should be similar between years. So far we have failed to provide any reason to explain such differences. Despite these differences, it seems that the artifacts of AVHRR and TMI do not generate great deviation in the InI estimation compared to that based on OI.v2 at an interannual scale. Note that the influences of cloud and rain on both sets of remote sensing data

Fig. 5. Interannual variability of SCSWP ArI and InI for TMI (a), AVHRR (b), and OI.v2 (c) in summer.
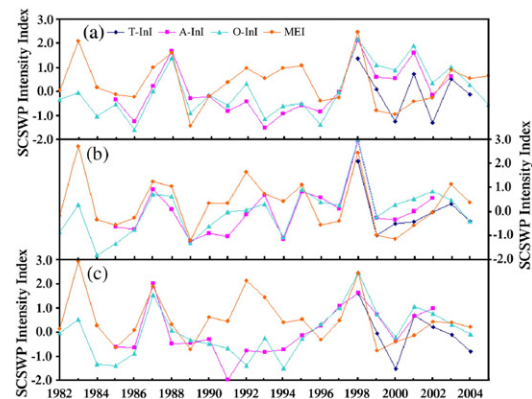

Fig. 6. Interannual variability of SCSWP InI for AVHRR, OI.v2 and TMI in spring (a), summer (b) and autumn (c), and comparison with MEI half a year before.

Table 5
Lag correlation coefficients between MEI and O-InI, A-InI and T-InI, respectively (0.707, 0.456 and 0.404 are 95% significant for 6 (TMI: 1998–2004), 17 (AVHRR: 1985–2002) and 22 (OI.v2: 1982–2004) degrees of freedom, respectively; values greater than 0.632 is boldfaced to emphasize statistical significance)

Lag (month)	T-InI			A-InI			O-InI		
	Spring	Summer	Autumn	Spring	Summer	Autumn	Spring	Summer	Autumn
−12	0.303	**0.893**	0.624	0.135	**0.644**	0.135	−0.063	**0.418**	0.236
−9	0.702	**0.922**	0.632	0.157	**0.609**	0.157	0.274	**0.533**	0.270
−6	0.687	**0.925**	0.686	0.268	**0.620**	0.268	0.280	**0.561**	0.310
−3	0.641	**0.984**	0.354	0.255	**0.617**	0.255	0.250	**0.516**	0.223
0	0.537	0.501	−0.260	0.062	0.186	0.062	0.153	0.156	−0.045
3	−0.022	−0.121	−0.184	−0.089	−0.162	−0.089	−0.180	−0.197	−0.112
6	−0.413	−0.150	−0.393	−0.300	−0.321	−0.300	−0.377	−0.248	−0.180
9	−0.418	−0.499	−0.360	−0.471	−0.438	−0.471	−0.336	−0.280	−0.354
12	−0.362	−0.521	−0.076	−0.485	−0.353	−0.485	−0.345	−0.282	−0.393

may be more serious in such a case because only seasonal mean data in a year are used instead of the multiyear mean data used in Section 3.1.

3.2.3. Correlation with ENSO

Lag-correlation coefficients between the three InIs in each season and MEI are shown in Table 5. All three InIs in summer are highly correlated with MEI at a time lag of 3 to 12 months. On the contrary, no significant correlationship is found in other seasons, while the correlation coefficients are relatively high at a time lag of 6 months. Comparison of the three InIs with MEI half a year before reveals that the main warming signals of the tropical Pacific occurring in 1987–1988 and 1997–1998 are all reflected in the InI patterns in each season (Fig. 6).

It has been suggested that the SCSWP primarily responds to the East Asian Monsoon forcing (Fu et al., 1994) and is relatively independent from the influence of its neighboring West Pacific (Zhou & Wang, 1999). Ekman pumping has also been invoked to be responsible for the interannual variability of the SCSWP (Zhu et al., 2003). Xie et al. (2003) pointed out that while delayed ENSO effect was a major mechanism for SCS variability, roughly half of the summer SST variance of the SCS possibly resulted from other processes such as internal variability of the SCS-western Pacific monsoon. Our results for three InIs consistently show the correct response of the SCSWP to the MEI in strong ENSO years, but not in normal years, and show that the SCSWP is most sensitive to the ENSO in summer. It seems probably that the SCSWP has its own rhythm modulated by local forcing, such as the East Asian monsoon, and it may be overwhelmed by delayed tropical Pacific ENSO signals when the ENSO signals are strong enough.

4. Summary and conclusion

In this paper, three SST datasets, AVHRR, TMI and OI.v2, are used to derive areal and intensity indices of SCSWP. Intensive comparison among them is carried out at monthly, seasonal and interannual scales, respectively.

Seasonal and monthly patterns of both ArI and InI derived from the three datasets are nearly identical; minor differences among InIs are observed in the period July to September. The interannual record of A-InI is significantly correlated with that of O-InI in each season for the period 1985 to 2002/2003, so

does T-InI with O-InI for the period 1998 to 2004. Differences between A-InI and O-InI mainly occur in autumn during the period 1990–1996.

The comparison between monthly records of ArIs and InIs shows that InIs peak in May to June and ArIs do in June to September, which is probably associated with changes of solar radiation, monsoonal forcing and summer upwelling. All three ArIs fluctuate from year to year in spring and autumn quite in accordance with InIs. However, in summer the consistency decreases, for example, O-InI and O-ArI do not vary in step with each other. It may be due to a stronger effect of coarse resolution of OI.v2 data on the index computation in summer, a season of high SST values, compared to other seasons.

Among the three seasons, only the InI in summer significantly correlated with MEI at a time lag of 3 to 12 months. Nevertheless, the main warming signals of the tropical Pacific occurring in 1987–1988 and 1997–1998 are also captured in the InI records in spring and autumn at a time lag of 6 months. It is suggested that the ENSO, in combination with local forcing such as the East Asian monsoon, may modulate the interannual variability of the SCSWP. The pattern driven by local forcing may be overwhelmed by delayed tropical Pacific ENSO signals when the ENSO signals are strong enough.

It is a fact that the three InIs are not fully consistent with each other at both monthly and interannual scale and nobody knows which one is the most convincing. It is possible that either the low resolution of OI.v2 or the cloud cover or effect of rain on the remote sensing data leads to important signals being missed. Guan and Kawamura (2004) have reported that it is very promising to generate high-resolution SST by merging infrared and microwave remote sensing data. Thus, merging of AVHRR and TMI may be a good solution for deriving high-quality SST time series and associated indices such as the SCSWP indices.

References

Barlow, M., Cullen, H., & Lyon, B. (2002). Drought in central and southwest Asia: La Niña, the warm pool, and Indian Ocean precipitation. *Journal of Climate, 15*(7), 697−700.

Chao, S. Y., Shaw, P. T., & Wu, S. Y. (1996). El Niño modulation of the South China Sea circulation. *Progress in Oceanography, vol. 38*. (pp. 51−93): Pergamon.

Chen, Y. M., & Qian, Y. F. (2005). Numerical study of influence of the SSTA in western Pacific Warm Pool on rainfall in the first flood period in south China. *Journal of Tropical Meteorology, 11*(1), 86−96 (in Chinese with English Abstract).

Fu, G., Zhou, F. X., Yu, S. Y., & Wang, D. X. (1994). On the mechanism of SST low frequency oscillation of the South China Sea. *Journal of Ocean University of Qingdao, 24*(4), 456−462 (in Chinese with English Abstract).

Guan, L., & Kawamura, H. (2004). Merging satellite infrared and microwave SST's — methodology and evaluation of the new SST. *Journal of Oceanography, 60*, 55905−55912.

Hayes, S. P., Chang, P., & Mcphaden, M. J. (1991). Variability of the sea surface temperature in the eastern equatorial Pacific during 1986–88. *Journal of Geophysical Research, 96*, 10553−10566.

He, Y. H., & Guan, C. H. (1999). A primary study of the South China Sea Warm Pool. *Plateau Meteorology, 18*(4), 595−602 (in Chinese with English Abstract).

Hoerling, M., & Kumar, A. (2003). The perfect ocean for drought. *Science, 299*, 691−694.

Huang, B. Y., & Mehta, V. M. (2004). Response of the Indo-Pacific Warm Pool to interannual variations in net atmospheric freshwater. *Journal of Geophysical Research, 109*(C06022). doi:10.1029/2003JC002114.

Jia, Y. L., Liu, Q. Y., & Sun, J. L. (2000). Seasonal characteristics of the South China Sea Warm Pool and numerical modeling. *Oceanologia et Limnologia Sinica, 31*(4), 354−362 (in Chinese with English Abstract).

Kilpatrick, K. A., Podesta, G. P., & Evans, R. H. (2001). Overview of the NOAA/ NASA Pathfinder algorithm for sea surface temperature and associated matchup database. *Journal of Geophysical Research, 106*, 9179−9198.

Kubota, M., Iwasaka, N., Kizu, S., Konda, M., & Kutsuwada, K. (2002). Japanese ocean flux data sets with use of remote sensing observations (J-OFURO). *Journal of Oceanography, 58*(1), 213−225.

Lehodey, P., Bertignac, M., Hampton, J., Lewis, A., & Picaut, J. (1997). El Niño Southern Oscillation and tuna in the Western Pacific. *Nature, 389*, 715−718.

Lehodey, P., Chai, F., & Hampton, J. (2003). Modeling climate-related variability of tuna populations from a coupled ocean-biogeochemical-populations dynamics model. *Fisheries Oceanography, 12*(4), 483−494.

Liu, Q. Y., Jiang, X., Xie, S. P., & Liu, W. T. (2004). A gap in the Indo-Pacific Warm Pool over the South China Sea in boreal winter: Seasonal development and interannual variability. *Journal of Geophysical Research, 109*(C7), 1029−1038.

Liu, Q. Y., Wang, D. Q., Jia, Y. L., Yang, H. Y., Sun, J. L., & Du, Y. (2002). Seasonal variation and formation mechanism of the South China Sea warm water. *Acta Oceanologica Sinica, 21*(3), 331−343.

McGregor, H., & Gagan, M. (1999). Tropical climate variability and the role of the Western Pacific Warm Pool: A review paper. *Quaternary Australasia, 16*(2), 24−27.

Mehta, V. M., & Fayos, C. (2004). Decadal–multidecadal variability of ENSO and its impacts on the global climate: Part I. The oceans. *CRCES Publication 2004-04*.

Mehta, V. M., & Mehta, A. V. (2004). Natural decadal–multidecadal variability of the Indo-Pacific Warm Pool and its impacts on global climate. *The CRCES-IPRC Workshop on Decadal Climate Variability, Hawaii*.

Nezlin, N. P., & McWilliams, J. C. (2003). Satellite data, empirical orthogonal functions, and the 1997–1998 El Niño off California. *Remote Sensing of Environment, 84*, 234−254.

Qu, T. D. (2000). Notes and correspondence upper-layer circulation in the South China Sea. *Journal of Physical Oceanography, 30*, 1450−1460.

Reynolds, R. W., Rayner, N. A., Smith, T. M., Stokes, D. C., & Wang, W. Q. (2002). An improved in situ and satellite SST analysis for climate. *Journal of Climate, 15*, 1609−1625.

Shaw, P. T., & Chao, S. Y. (1994). Surface circulation in the South China Sea. *Deep-Sea Research. Part 1. Oceanographic Research Papers, 41*, 1663−1683.

Shaw, P. T., Chao, S. K., Liu, K. K., Pai, S. C., & Liu, C. T. (1996). Winter upwelling off Luzon in the northeast South China Sea. *Journal of Geophysical Research, 101*, 16435−16448.

Sun, D. Z. (2003). A possible effect of an increase in the Warm-Pool SST on the magnitude of El Niño warming. *Journal of Climate, 2*, 185−205.

Udarbe-Walker, M. J. B., & Villanoy, C. L. (2001). Structure of potential upwelling areas in the Philippines. *Deep-Sea Research. Part 1. Oceanographic Research Papers, 48*, 1499−1518.

Wang, Q. (2003). The study of the seasonal and interannual variations of the South China Sea warm water. *Journal of Ocean University of Qingdao, 33*(6), 821−824 (in Chinese with English Abstract).

Weier, J. (2001). Reverberations of the Pacific Warm Pool. Available at: http:// earthobservatory.nasa.gov/Study/WarmPool/

Wentz, F. J., Gentemann, C., Smith, D., & Chelton, D. (2000). Satellite measurements of sea surface temperature through clouds. *Science, 288*, 847−850.

Wyrtki, K. (1961). Physical oceanography of the Southeast Asian waters: Scientific results of marine investigations of the South China Sea and the Gulf of Thailand 1959–1961. *NAGA Report*, Vol. 2 (pp. 195). Scripps Institute Of Oceanography, La Jolla: University of California Press.

Xie, S. P., Xie, Q., Wang, D. X., & Liu, W. T. (2003). Summer upwelling in the South China Sea and its role regional climate variations. *Journal of Geophysical Research, 108*(C8), 3261−3273.

Yu, J., Mechoso, C. R., McWilliams, J. C., & Arakawa, A. (2002). Impacts of the Indian Ocean on the ENSO cycle. *Geophysical Research Letters, 29*(8), 1204−1207.

Zhang, Q. R., Du, Y., & Wang, D. X. (2001). Shape features of warm water in South China Sea. *Journal of Tropical Oceanography, 20*(1), 69−76 (in Chinese with English Abstract).

Zhao, Y. P., & Chen, Y. L. (2001). Seasonal and inter-annual variability of the South China Sea Warm Pool and its relation to the South China Sea monsoon onset. *Journal of Tropical Meteorology, 7*(1), 19−28.

Zhou, F., & Wang, J. T. (1999). Phase discontinuity of the SST interannual oscillation between the South China Sea and its adjoining West Pacific Region. *Oceanologia et Limnologia Sinica, 30*(6), 679−686 (in Chinese with English Abstract).

Zhu, X. H., Wang, W. Q., Zhou, W. D., Wang, D. X., & Xie, Q. (2003). Interannual mode of sea surface temperature in relation to monsoon forcing in South China Sea. *Journal of Tropical Oceanography, 22*(4), 42−50 (in Chinese with English Abstract).